P. J. Phys. 02 (01), 042 (April 2026) PANE Journal of Physics

ETCHING CHARACTERISTICS OF LR-115 TYPE II FILMS USING PERCENTAGE–TRACK DENSITY

Yubaraj Sharma[1], Budmiki Talang[2], Deveshwori Maibam[3], and Aibanjop Pyngrope*[4]

[1]*Department of Physics, Don Bosco College, Tura, Meghalaya, India*
[2]*Department of Physics, Assam Don Bosco University, Sonapur, Assam, India*
[3]*Don Bosco College of Teacher Education, Tura, Meghalaya, India*
[4]*Department of Physics, Captain Williamson Sangma State University, Meghalaya, India*

*Corresponding Author: ibanbiba@gmail.com

(Received 26 September 2025; revised 21 November 2025; accepted 11 December 2025; published 6 April 2026)

Abstract: We investigate the etching characteristics of environment-exposed LR-115 film (cellulose nitrate) solid state nuclear track detector (SSNTD), which is commonly used for the detection of terrestrial ionizing radiation, particularly in indoor and soil gas environments. The percentage-track density in exposed LR-115 detectors is used as a proxy for bulk etching and examined under different etching conditions. Expectedly, results reveal that the track density increases with temperatures and normality. Linear regression coefficients as well as multiple linear regression coefficients are estimated.

Keywords: SSNTD; Etching; LR-115, Regression

PACS: 07.57.Kp, 29.40.-n; 87.53.Bn; 87.53.-j

1 Introduction

Solid State Nuclear Track Detectors (SSNTDs) are widely used for detecting and measuring properties of fast-moving charged particles, including alpha particles, fission fragments, and heavy ions, owing to their remarkable sensitivity, durability, and affordability [1]. Among SSNTDs, polymeric detectors stand out due to their sensitivity, and among polymeric detectors, the cellulose nitrate polymer film, commonly known as LR-115 (type II), is the most favoured for monitoring environmental radioactivity, especially in studies on radon and thoron concentration [2–5]. These detectors capture ionizing radiation by creating latent tracks, which can be uncovered via an appropriate chemical etching process [1].

The etching process is vital for visualizing and analysing these tracks. Factors like etching time, temperature, and the concentration of the etchant greatly influence track geometry, etch rate, and consequently, track density measurements [1, 6, 7]. Therefore, a comprehensive understanding of etching characteristics is crucial for precise particle identification as well as dosimetric calculations. Although morphology of etch pits conveys details about the energy and charge of the incident particle, it is the simpler quantity — track density — that is useful for measurement of environmental radioactivity [8–10]. Several researchers have focused on optimizing etching conditions to enhance the resolution and accuracy of the LR-115 detector response. For instance, Durrani and Bull [1] provided foundational insights into track formation and etching mechanisms, while later studies have explored variations in chemical etchants and etching protocols to improve track contrast and reduce background noise [7, 11, 12]. These advancements also warrant corresponding investigations to corroborate the etching behaviour of LR-115 films under different controlled exposures and chemical conditions.

The present study focuses on examining the etching properties of exposed LR-115 film, particularly how various etching parameters affect track revelation. It is usually the bulk etch rate of detectors that is measured against etching parameters, but during use in the field, it is the track density that is directly measured and hence its adoption in the present study. Such investigations are essential for enhancing the accuracy of SSNTD-derived measurements, particularly in situations involving low-level radiation monitoring.

2 Materials and method

In the present study, LR-115 type II SSNTD manufactured by DOSIRAD, France, with an active layer of $12\,\mu\mathrm{m}$ and polyester base of thickness $100\,\mu\mathrm{m}$ was used. The water-bath used had a thermostat with control of $\pm 2^\circ\mathrm{C}$. A typical microscope (Labomed) with magnification $40\times$ was used for counting and measurement of track properties. For etching, laboratory-grade NaOH was used. For radiation source, we used the ubiquitous environmental radioactivity — the detectors were hung from threads for a period of 90 days, similar to the method of bare-mode exposure for the measurement of indoor radon concentration [13, 14].

The primary objective of the study is to determine etching characteristics in terms of track densities observed in the etched LR-115 film by varying etching duration, etchant concentration and etching temperature. Two etchant concentrations were identified for the experiment, viz., 2N and 2.5N of NaOH; three temperature values were identified, viz., $40^\circ\mathrm{C}$, $50^\circ\mathrm{C}$ and $60^\circ\mathrm{C}$, while the track densities were measured at four etching durations, viz., 60, 70, 80 and 90 minutes. These values of the parameters were chosen keeping in mind the upper limits of standard procedure of etching LR-115 films, which are 2.5N, $60^\circ\mathrm{C}$ and 90 minutes [10, 15, 16]. The raw values of track density are not conducive for direct calculation as they are highly dependent on the exposure duration and the concentration of alpha-emitting radon atoms in air. Therefore, with the assumed standard values of etching parameters, we represent track density in percentage terms with respect to the track density obtained for 90 minutes of etching at $60^\circ\mathrm{C}$ and 2.5N etchant solution.

The exposed detectors were selected randomly and placed into six groups labelled with a specific normality value and temperature. Successive etching was carried out, keeping step with the time interval chosen for the study. The etching process is carried out by placing a conical beaker with the etchant of a specific concentration in the thermostatically controlled water bath at specific temperature. When the temperature of the etching solution reaches equilibrium with the temperature of the water bath, the LR-115 films are introduced in the beaker so as to completely submerge them in the etchant. At specified intervals, the LR-115 films are extracted from the water bath and dried. The track densities in the etched films are then determined by manually counting the tracks with the help of the microscope.

Linear regression as well as multiple linear regression were carried out to estimate a linear relationship between the response (or dependent) variable, viz., the track density, and three explanatory (or independent) variables — etchant normality, etchant temperature and etching time. The linear regression was done using the `scikit-learn` package [17], while the multiple regression was done using the R programming language [18].

A simple linear regression consists of a single response as well as a single explanatory variable and entails the estimation of the coefficients of the linear equation (usually called the prediction equation) of the form [19],

$$y = \beta_0 + \beta_1 x + \varepsilon \tag{1}$$

where $\hat{y}$ is the predicted value for a given value of the explanatory variable x (the cap over a variable indicates predicted or estimated value); $\hat{\beta}_0$ and $\hat{\beta}_1$ are respectively the intercept and slope of the linear relationship, and ε is the error (the unpredictable part of the data).

Multiple linear regression extends linear regression to accommodate multiple explanatory variables $(x_1, x_2, \cdots, x_k)$ for a single response variable (y) and is mathematically expressed as [19],

$$y = \beta_0 + \beta_1 x_1 + \beta_2 x_2 + \cdots + \beta_k x_k + \varepsilon. \tag{2}$$

The other symbols in the above equation have meanings similar to those used in equation (1).

We do realise that the results of this study have limited generality due to the limited range of variables considered; however, this study can pave the way for more detailed experimental setup and analysis.

3 Results and Discussions

The obtained experimental values of percentage track density are plotted as a function of etching time for different values of etching temperature in the two subplots given in figure 1. Each subplot in the figure represents data corresponding to a specific etchant normality — 2N and 2.5N. We have kept the y-axis of both the subplots the same to facilitate comparison at the cost of some detail. Expectedly, track densities increase with time as well as temperature. It is also seen that the general trend indicates higher slopes for higher temperatures. Track densities are also higher for higher normality for a given etching time, thus indicating throughout a positive correlation between track density and all three explanatory variables.

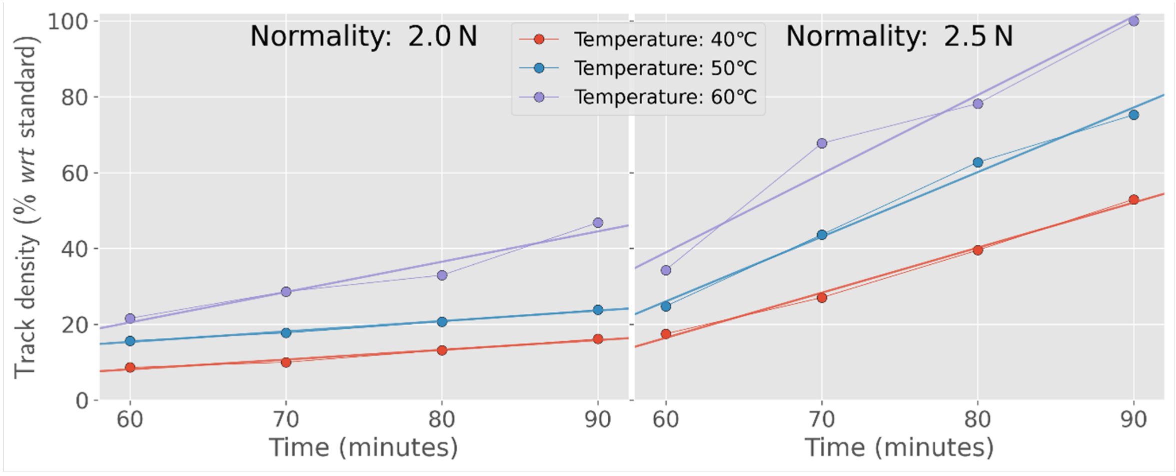

Figure 1: Track density in LR-115 as a function of etching time for various etching temperatures for two different normalities of etchant concentration. Solid lines of corresponding colour indicate linear-fit line.

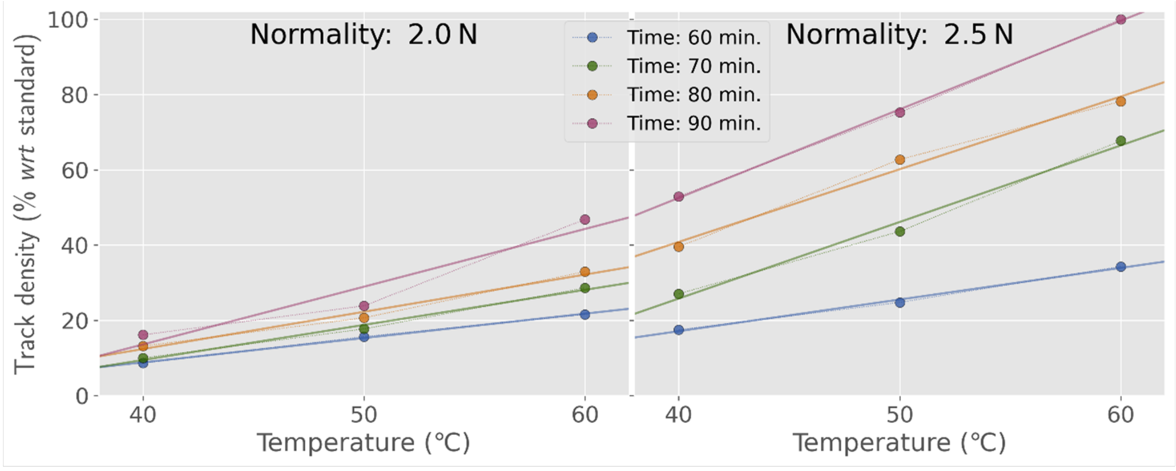

Figure 2: Track density in LR-115 as a function of etching temperature for different etching times for two different normalities of etchant concentration. Solid lines of corresponding colour indicate linear-fit line.

To highlight the effect of etching temperature, we have replotted the data in figure 2, but with the temperature on the x-axis. This is to visually show the effect of temperature on track density at various etching times.

To quantify the trend across the various variables, we have provided the values of linear regression in table 1, along with corresponding goodness-of-fit parameters.

Table 2 provides the value of coefficients for the various explanatory variables obtained from a multiple regression exercise carried out on the experimental data. The Sum of Squared Errors (SSE) for the regression is found to be 1779.188 and the multiple R^2 value is 0.8719. We can see that the R^2 value of the multiple regression is noticeably lesser than the R^2 value of direct linear regression (table 1), indicating that the generalization of the fit to multiple variables reduces the goodness-of-fit observed in individual regressions.

Based on the coefficients given in table 2, the percentage track density (ρ) as a function of time of etching in minutes (t), the temperature in $^\circ$C (θ) and the normality of etchant (N) can be written as [1] (c.f., equation 2),

$$\rho = -250.38 + 1.05\,t + 1.41\,\theta + 61.29\,N. \tag{3}$$

Based on the value of coefficients obtained, we find that, in terms of numerical value (with the specific units used here), the normality has the highest impact (as it has the highest value of slope, thus providing a large increase in the value of dependent variable for a specified increase in its value), followed by temperature and then

---

[1] Rounded to two decimal digits

Normality	Time	Temperature	Slope	Intercept	SSE	r^2
2	60	**	0.65	-17.1	0.22	0.997
2	70	**	0.93	-27.8	1.69	0.990
2	80	**	0.99	-27.2	3.80	0.981
2	90	**	1.53	-47.8	38.64	0.924
2.5	60	**	0.84	-16.5	0.86	0.994
2.5	70	**	2.03	-55.6	9.38	0.989
2.5	80	**	1.93	-36.4	9.95	0.987
2.5	90	**	2.35	-41.6	1.04	0.999
2	*	40°C	0.26	-7.3	0.84	0.975
2	*	50°C	0.27	-1.1	0.35	0.991
2	*	60°C	0.80	-27.5	19.15	0.944
2.5	*	40°C	1.19	-54.9	3.94	0.994
2.5	*	50°C	1.70	-76.2	12.45	0.992
2.5	*	60°C	2.07	-85.6	92.47	0.959

* indicates all values of etching time variable, viz., 60, 70, 80 and 90 minutes.

** indicates all values of etching temperature variable, viz., 40°C, 50°C and 60°C.

Table 1: Coefficients of linear regression between normality–etching time and normality–temperature along with goodness-of-fit statistics.

Coefficients	Estimate	Std. Error	p-value
Constant term (or intercept)	-250.3835	24.6930	2.50×10^{-9}
Time (minutes)	1.05	0.1722	5.85×10^{-6}
Temperature (°C)	1.4077	0.2358	7.74×10^{-6}
Normality	61.2879	7.7011	1.260×10^{-7}

Table 2: Coefficients of multiple linear regression for the response variable of track density and the three etching parameters.

the time of etching. For example, equation (3) predicts that an increase in normality by ΔN would produce about $(60\,\Delta N)\%$ more tracks compared to a $\Delta\theta$ increase in temperature.

It is hoped that the calculations and regression values provided here might prove useful in numerical simulation exercises and facilitate comparison even under different etching conditions.

Conclusions

Experimental values of percentage track densities for the solid-state nuclear track detector LR-115 type II for various etching conditions are presented. The observed trends are consistent with those reported in literature [1, 8]. Linear and multiple linear regression coefficient values are estimated.

References

[1] S. A. Durrani and R. K. Bull, *Solid State Nuclear Track Detection: Principles, Methods and Applications*, International Series in Natural Philosophy, Vol. 111 (Pergamon Press, Oxford, 1987).

[2] A. Pyngrope, P. Sangma, and R. K. Kakati, Journal of Physics: Conference Series **2919**, 012039 (2024).

[3] L. A. S. Pereira and C. A. T. Sáenz, Physics **7**, 56 (2025).

[4] P. Pereyra, C. J. Guevara-Pillaca, R. Liza, B. Pérez, J. Rojas, L. Vilcapoma L., S. Gonzales, L. Sajo-Bohus, M. E. López-Herrera, and D. Palacios Fernández, Atmosphere **14** (2023).

[5] A. S. Hussein, Radiation Environment and Medicine **10**, 26 (2021).

[6] S. Durrani and P. Green, Nuclear Tracks and Radiation Measurements (1982) **8**, 21 (1984).

[7] M. Caresana, F. Campi, and M. Ferrarini, Radiation Protection Dosimetry **113**, 354 (2005).

[8] D. Nikezic, F. Ng, and K. Yu, Applied Radiation and Isotopes **61**, 1431 (2004).

[9] V. Mehta, C. Kapil, D. Shikha, and S. Kanse, Environmental Monitoring and Assessment **196**, 128 (2024).

[10] K. Eappen and Y. Mayya, Radiation Measurements **38**, 5 (2004).

[11] D. Palacios, L. Sajo-Bohus, H. Barros, E. Greaves, and F. Palacios, Revista Mexicana de Física **56**, 22 (2010).

[12] M. D. Salim, N. F. Kadhim, and A. A. Ridha, AIP Conference Proceedings **2290**, 030039 (2020).

[13] M. S. Khan, Journal of Nuclear and Radiation Sciences **1**, 19 (2022).

[14] D. Maibam, Y. Sharma, A. K. Dewsaw, A. Kenye, D. Walia, and A. Saxena, Journal of Applied and Fundamental Sciences **1**, 130 (2015).

[15] J. Virk and H. S. Virk, Research Reviews: A Journal of Toxicology **11**, 7 (2021).

[16] M. Prasad, M. Rawat, A. Dangwal, M. Yadav, G. S. Gusain, R. Mishra, and R. C. Ramola, Radiation Protection Dosimetry **167**, 102 (2015).

[17] F. Pedregosa, G. Varoquaux, A. Gramfort, V. Michel, B. Thirion, O. Grisel, M. Blondel, P. Prettenhofer, R. Weiss, V. Dubourg, J. Vanderplas, A. Passos, D. Cournapeau, M. Brucher, M. Perrot, and Édouard Duchesnay, Journal of Machine Learning Research **12**, 2825 (2011).

[18] R Core Team, *R: A Language and Environment for Statistical Computing*, R Foundation for Statistical Computing, Vienna, Austria (2025).

[19] L. Ott and M. Longnecker, *An Introduction to Statistical Methods and Data Analysis*, 7th ed. (Cengage Learning, 2016).